Hindawi
Advances in Civil Engineering
Volume 2018, Article ID 5796086, 9 pages
https://doi.org/10.1155/2018/5796086

Research Article

Crack Characteristic and Permeability Change of Compacted Clay Liners with Different Liquid Limits under Dry-Wet Cycles

Yong Wan[1], **Qiang Xue**[1], **Lei Liu**[1] and **ShanYong Wang**[2,3]

[1]*State Key Laboratory of Geomechanics and Geotechnical Engineering, Institute of Rock and Soil Mechanics, Chinese Academy of Sciences, Wuhan 430071, China*
[2]*ARC Centre of Excellence for Geotechnical Science and Engineering, Civil, Surveying and Environmental Engineering, The University of Newcastle, Callaghan, NSW 2308, Australia*
[3]*State Key Laboratory of Hydraulics and Mountain Engineering, College of Water Resource and Hydropower Engineering, Sichuan University, Chengdu 610065, China*

Correspondence should be addressed to Yong Wan; ywan@whrsm.ac.cn

Received 26 September 2018; Accepted 5 November 2018; Published 26 November 2018

Academic Editor: Flavio Stochino

The crack characteristic and permeability change in six compacted clay liners (CCLs) under dry-wet cycles were studied. Results show that as soil liquid limit (LL) increases, the crack block (CB) number, crack ratio (CR), and crack length (CL) of the CCLs increase under the dry state. The CB sizes of all the six CCLs correspond to normal distribution. A piecewise linear relationship exists between crack parameters and soil LL, and the slope at LL < 50 is larger than the slope at LL > 50. The size of the representative elementary volume (REV) of cracked CCL decreases linearly with the increase in soil LL when LL < 50. The linear fitting result is REV = 90.5 – 1.6 LL, whereas REV change is inconspicuous with a mean value of approximately 10 cm when LL > 50. The sample size of the CCLs for the permeability test must be larger than REV. Before and after three dry-wet cycles, the permeability ratio (K_3/k_0) initially increases and eventually decreases as soil LL increases, and LL at the peak value of K_3/k_0 is 36.1%. However, linear relationships exist between permeability D-value ($K_3 - k_0$) and soil LL in a semilog coordinate system when LL < 50%, whereas the change in the permeability D-value is inconspicuous with a mean value of approximately 1.67×10^{-8} cm/s when LL > 50%. The volume and mean width of unclosed cracks are two main factors that determine the increase in permeability after dry-wet cycles. After three dry-wet cycles, these factors decrease as soil LL increases, thereby reducing the permeability D-value.

1. Introduction

A final cover prevents the infiltration of rainwater and the volatilization of noxious fumes after a landfill is filled with garbage [1, 2]. Compacted clay liners (CCLs) are widely used as final covers for landfills given their ultralow permeability characteristics. However, this type of clay cover is easily affected by seasonal dry-wet cycles because it is placed on a landfill surface as the final cover. Studies have shown that numerous cracks initiated on the clay cover after seasonal dry-wet cycles [1, 3–5]. These cracks provide direct channels for rainwater infiltration and threaten the safe operation of a landfill site [1, 6, 7].

The effect of dry-wet conditions on CCLs is closely related to clay properties. Othman et al. [8] showed that the clay permeability coefficient increased with the increase in the liquid limit (LL) under dry-wet cycles. Brian and Benson [9] studied the soil LL effect on the shrinkage strain characteristics of natural clays, which showed that as LL increased, clay shrinkage strain would also increase. Meanwhile, the existence of a contraction crack can increase the soil permeability coefficient from 1 to 3 orders of magnitude. However, Rayhani et al. [10, 11] found that when clay LL was low or high, the increment of the CCL permeability coefficient under dry-wet cycles was not evident.

The accurate testing of the CCL permeability coefficient is critical to evaluate the effect of the dry-wet cycle on CCL antiseepage capacity. Drumm et al. [12] discussed the crack soil permeability coefficient of different areas and confirmed the nonuniform damage characteristics of a CCL structure under dry-wet cycles. Omidi et al. [13] compared the results of a permeability coefficient test via a flexible wall penetration experiment (10 cm in the specimen diameter) and a field double-ring infiltration experiment. The results showed that the flexible wall penetration experiment underestimated soil permeability increase under the dry-wet cycle condition. Rayhani et al. [10, 11] conducted the soil infiltration test research on a large crack (30 cm in the specimen diameter) and compared the sample size effect on the coefficient of permeability of the CCL. Wan et al. [3] found that the boundary effect of crack soil also affected the permeability test precision even if CCL size was larger than 30 cm. Li and Zhang [14] analyzed CCL shrinkage cracking characteristics, determined the relationship between the REV and cracking space, length, and other parameters, and indicated that the sample size of the cracked CCL for the permeability test must be larger than REV.

The internal mechanism of the increase in the CCL permeability coefficient is its macro-micro structural damage under dry-wet cycles. Research indicates that a change in the CCL permeability coefficient can be attributed to the existence of unclosed cracks in CCLs after wet-dry cycles [3–5, 15]. However, crack space is relatively small under the saturation condition than under the dry condition; thus, conducting quantitative observation is difficult. Many studies have used the CCL surface crack rate under the dry condition to indirectly evaluate the crack effect of soil permeability under dry-wet cycles. Xue et al. [4, 5, 11, 14, 16, 17] showed that the shrinkage crack number, area, and length in unit area increased, whereas the permeability ratio initially increased and then decreased with the increase in soil LL, thereby indicating that no direct relationship existed between the change in CCL permeability and crack area under the dry condition. The unclosed cracks in a CCL is attributed to the soil pore volume shrinkage of the CCL, which cannot fully recover again after saturation, and the unclosed crack volume can be calculated using the total soil pore volume decrease under the dry-wet cycle condition [3, 15].

In the present study, the shrinkage crack characteristics of six CCLs with different LLs is determined through a CCL cracking test, and the relationship between the representative elementary volume (REV) and LL of CCLs is established after several dry-wet cycles. The result of the permeability coefficient test shows that CCL sample size is larger than REV before and after three dry-wet cycles, and the relationship between permeability coefficient increment and LL is established after the dry-wet cycles. Lastly, the structural damage of the CCLs was determined via the mercury intrusion porosimetry (MIP) test. The aforementioned results can provide the parameters for the safety evaluation of landfill CCL impervious structure.

2. Materials and Methods

2.1. Experimental Materials. Clay content is the decisive factor of soil LL. The mixing of soils with different clay contents is a common method used to obtain different soil LLs in existing studies about the relationship between soil engineering properties and LL [11]. In the current study, six soil samples with different LLs were obtained by mixing two natural soil samples (Soil A and Soil B) with different mass ratios. Soil A, which was collected from Wuhan City, had a low soil LL and a clay content of 8.44%. Soil B, which was collected from Xinyang City, had a high soil LL and a clay content of 63.99%. The mass ratios of Soil B in the six mixed soil samples were 0, 12.5%, 25%, 37.5%, 50%, and 100%, which were labeled Soil #1 to Soil #6, respectively. The physical parameters and mineral composition of Soil #1 to Soil #6 are shown in Tables 1 and 2, respectively.

2.2. Experimental Methods

2.2.1. Production of CCL Samples for the Cracking Test. After air-drying, crushing, and sifting the soil through a 2 mm size sieve, the two natural soil samples were mixed following the aforementioned mass ratios. Then, the moisture contents of the six mixed soil samples were adjusted to 20% by spraying water. After 24 h, the mixed soil was layered and pressed into a rectangular steel box with an inner dimension of 56 cm (length) × 46 cm (width) × 10 cm (depth). The six CCLs have the same thickness of 5 cm and the same dry density of 1.5 g/cm^3.

2.2.2. Simulation of the Dry-Wet Cycle. After compacted molding, the CCLs were soaked/saturated for 72 h in the rectangular steel box and then placed in a dryer at 50°C for 72 h. The aforementioned steps were repeated thrice. After each trial, the cracks on the CCL surface were recorded using a digital camera.

2.2.3. Analysis of Cracks on the CCL Surface. The image processing functions in MATLAB were used to analyze the crack characteristics of CCL. The box boundary was wiped off from the original images, and the clipped images were transformed into binary images (black represented the crack area, whereas white represented the noncrack area). The crack ratio (CR) and crack length (CL) could be obtained from the statistics of the black area and the crack skeleton line length in a unit of the statistical area. A crack block (CB) is a closed crack skeleton line.

The REV of the CCLs with cracks is the smallest unit that can contain whole crack messages. When unit size is higher than some values, the relative error of crack characteristic parameters is always less than the allowable relative error, and the smallest unit size is the REV size [14]. In this paper, choose CR as the mainly parameter of crack characteristic, and the CR relative error of the random statistical zone can be solved as follows:

Table 1: Soil physical properties.

Soil number	Specific gravity, Gs	Plasticity limit (%)	Liquid limit (%)	Plasticity index	Clay content (%)	Soil type
Soil #1	2.72	19.5	33.6	14.1	8.44	CL
Soil #2	2.71	19.8	36.1	16.3	15.38	CL
Soil #3	2.70	20.4	41.2	20.8	22.33	CL
Soil #4	2.69	21.2	47.2	26.0	29.27	CL
Soil #5	2.68	22.5	66.6	44.1	36.21	CH
Soil #6	2.66	33.2	99.6	66.4	63.99	CH

Table 2: Soil mineral composition.

Soil number	Mineral composition (%)				
	Quartz	Albite	Illite	Montmorillonite	Kaolinite
Soil #1	77.74	13.91	1.64	4.70	2.01
Soil #2	71.66	13.02	2.92	10.35	2.04
Soil #3	65.58	12.13	4.20	16.00	2.07
Soil #4	59.5	11.25	5.48	21.64	2.10
Soil #5	53.42	10.36	6.76	27.29	2.12
Soil #6	29.10	6.82	11.87	49.88	2.24

$$\delta_{\mathrm{CR}}(\mathrm{z}) = \frac{\mathrm{CR}(z)}{\mathrm{CR}_T} \times 100\%, \tag{1}$$

where CR_T is the crack ratio that statistics the whole CCL sample, $\mathrm{CR}(z)$ is the crack ratio that statistics the random statistical zone with a diameter of CR.

2.2.4. Testing CCL Permeability. After drying thrice for 72 h, the CCLs were soaked/saturated for 24 h in the rectangular steel box and then cut into round samples with a diameter of 30 cm for the permeability test (Figure 1). The permeability test used a PN3230M environmental soil flexible wall permeameter, manufactured by the American company GeoQuip. The permeability test properties included back pressure saturation for 24 h with an ambient pressure of 20 kPa and then permeation for 48 h with an ambient pressure of 80 kPa and an osmotic pressure of 40 kPa.

2.2.5. MIP Test. A small CCL, with a diameter of 6.18 cm and a thickness of 2 cm, was used for the MIP test. The homogeneity of this small CCL was more than that of a large CCL in the rectangular box. With the exception of sample size, the other conditions are the same as those for a large CCL. Before and after three dry-wet cycles, three types of small CCLs (Soil #1, Soil #3, and Soil #5) were used for the MIP test. The MIP test method was presented by Wan et al. [3].

3. Results and Analysis

3.1. Analysis of the Crack Characteristics in the CCLs

3.1.1. Crack Characteristic Test Results of the CCLs. Figure 2 shows the images of the crack characteristics in the six CCLs after three dry-wet cycles. The crack characteristic parameters are shown in Table 3. For the CCL with low LL (LL < 50%), only a few cracks appear on the CCL surface (Soils #1–#3). As soil LL increases, CR and CL also gradually increase. When LL is close to (Soil #4) or over 50% (Soils #5 and #6), the crack on the CCL surface is close set and uniform.

3.1.2. Relationship between Cracking Parameters and LL. Figure 3 shows the relationship between CCL crack characteristic parameters and soil LL. With a demarcation point of 50% LL, a piecewise linear relationship exists between crack characteristic parameters and soil LL, and the slope at LL < 50 is larger than that at LL > 50. The piecewise linear fitting results are as follows:

$$\begin{cases} \mathrm{CL} = -41.42 + 1.34\mathrm{LL}, & \mathrm{LL} < 50\%, \\ \mathrm{CL} = 7.92 + 0.12\mathrm{LL}, & \mathrm{LL} > 50\%, \\ \mathrm{CR} = -23.51 + 0.73\mathrm{LL}, & \mathrm{LL} < 50\%, \\ \mathrm{CL} = 3.43 + 0.04\mathrm{LL}, & \mathrm{LL} > 50\%. \end{cases} \tag{2}$$

3.1.3. Relationship between CB Parameters and LL. The frequency of CB size can be calculated using the following formula:

$$F(d) = \frac{N(d - 0.5\delta, d + 0.5\delta)}{N \times \delta}, \tag{3}$$

where N is the total CB number of each CCL, $N(d - 0.5\delta, d + 0.5\delta)$ is the number of CB with a size of $[d - 0.5\delta, d + 0.5\delta]$, and δ is the space length.

Figure 4 shows the CB size probability distribution and its fitting results with a normal distribution function. The fitting parameters are shown in Table 4. The normal distribution relationship between size and number is evident except for Soil #1 because of its extremely small CB number.

Figure 5 shows the relationship between the normal distribution parameters (i.e., the expectancy value and mean square error) of CB size and soil LL. The expectancy value and mean square error decrease sharply with an increase in LL for low LL clays; both parameters exhibit apparent linear relationships with LL. The fitting equation is given as Equation (5). The expectancy value and mean square error are reduced slightly when soil LL is higher than 50%, and the change is not evident:

$$\begin{cases} \mu = 57.7 - 1.11\mathrm{LL}, \\ \sigma = 17.5 - 0.32\mathrm{LL}. \end{cases} \tag{4}$$

3.1.3. Relationship between REV and LL. Figure 6 shows the relative error of CR with an increase in statistics zone size.

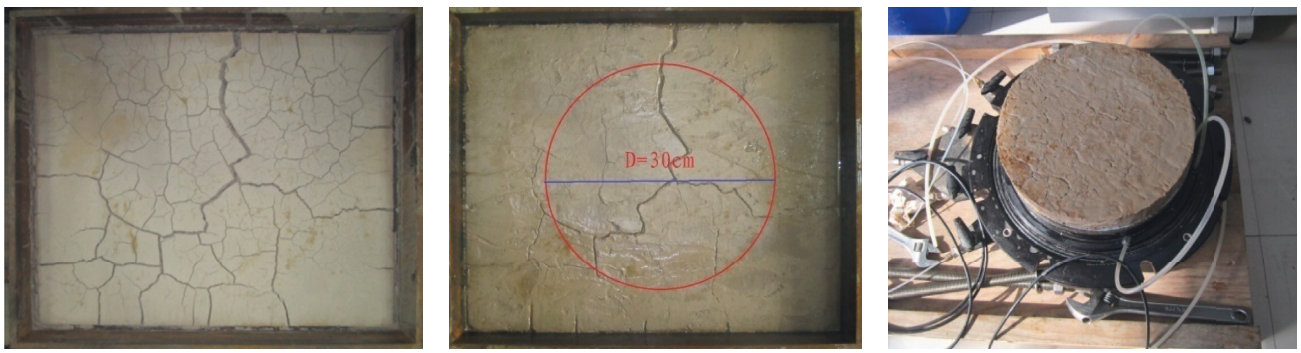

(a) (b) (c)

Figure 1: Process of dry-wet cycles and infiltration test: (a) three times drying; (b) saturation again; (c) permeability test.

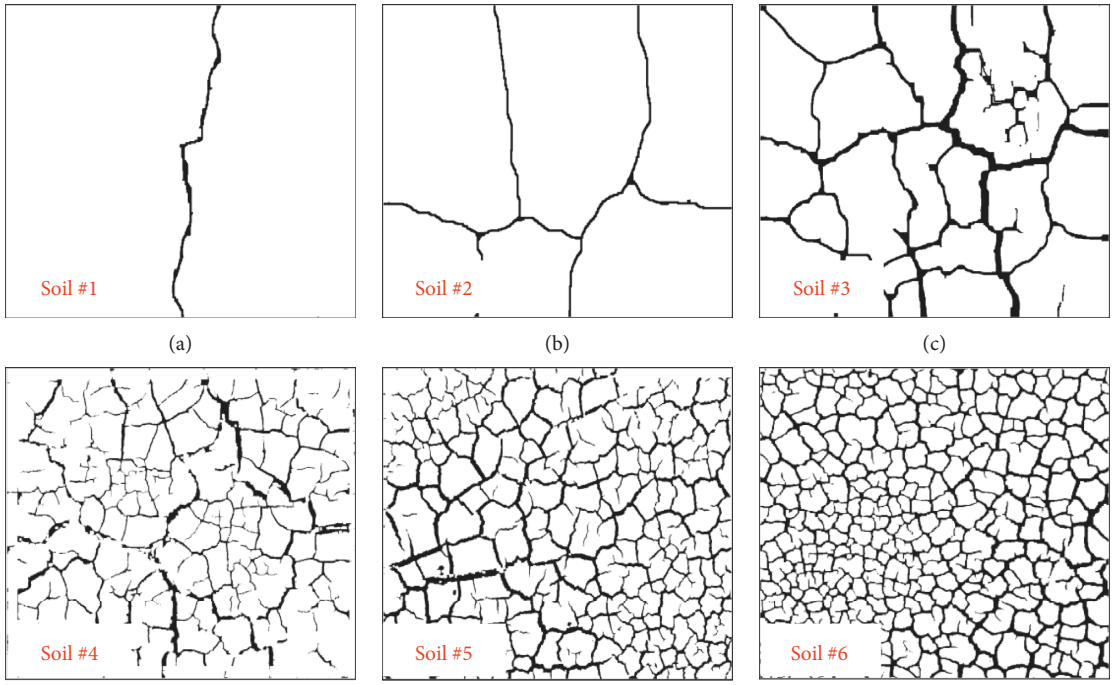

(a) (b) (c)

(d) (e) (f)

Figure 2: Shrinkage cracking test results of the six types of CCLs. (a) Soil #1. (b) Soil #2. (c) Soil #3. (d) Soil #4. (e) Soil #5. (f) Soil #6.

Table 3: Cracking characteristic parameters of the six CCLs.

Soil number	Crack parameters		Crack block parameters		
	CR (%)	CL (m^{-1})	Number	Mean area (cm^2)	Mean size (cm)
Soil #1	1.26	4.43	2	1190.2	34.5
Soil #2	1.92	5.58	6	400.0	20.0
Soil #3	7.66	15.15	19	125.4	11.2
Soil #4	10.48	21.60	98	125.4	4.9
Soil #5	17.44	31.47	305	24.0	2.8
Soil #6	19.55	35.90	421	5.3	2.3

The relative error volatility of CR changes as statistics zone size increases, but the change range decreases with an increase in statistics zone size. When statistics zone size is larger than some values, the relative error is smaller than 10% but larger than −10%. The minimum statistics zone size (filled dots in Figure 6) is REV size.

Figure 7 shows the relationship between REV and soil LL. For low soil LL, REV decreases linearly with an increase in soil LL; the linear fitting results are shown in Equation (5). For high soil LL, REV decreases slightly as LL increases. Hence, setting REV as 10 cm for high liquid limit soil is appropriate:

$$\mathrm{REV} = 90.5 - 1.6\mathrm{LL}. \quad (5)$$

3.2. Analysis of Pore Size Distribution (PSD) in CCLs

3.1.1. PSD Test Result. Figure 8 shows the PSD in the CCLs before (DW0) and after three dry-wet cycles (DW3). The

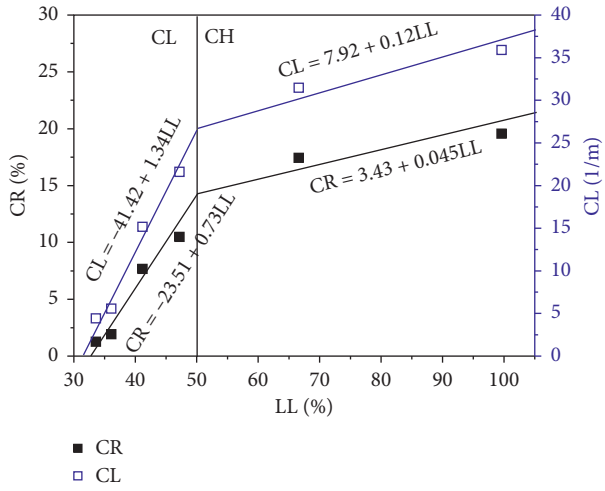

Figure 3: Relationship between CCL crack parameters and soil LL.

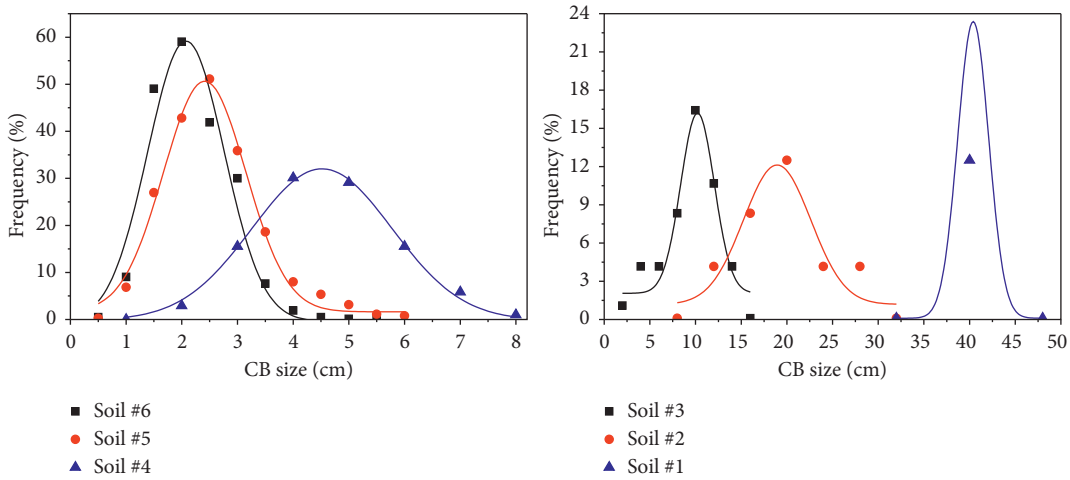

Figure 4: Probability distribution of CB size and its normal distribution fitting results.

Table 4: Normal fitting parameters of CB size probability distribution.

Soil number	Crack block number	Space length, δ (cm)	Expectancy value, μ	Mean square error, σ	Correlation coefficient
Soil #1	2	8	40.4	3.4	0
Soil #2	6	4	18.9	7.4	0.78
Soil #3	19	2	10.3	3.7	0.90
Soil #4	98	1	4.5	2.5	0.99
Soil #5	305	0.5	2.4	1.5	0.98
Soil #6	421	0.5	2.0	1.4	0.94

bimodal PSD curves have pore sizes of 0.1, 6, and 80 μm in three troughs. We classify soil pores into three categories based on the classification method of soil pore size in the existing research [3, 18]: large pores (>6 μm), medium pores (6 to 0.1 μm), and small pores (<0.1 μm).

3.2.2. PSD in CCLs before Dry-Wet Cycles. Figure 9 shows the different types of pore volume of three CCLs at DW0. The PSD in CCLs differs at DW0 because of the varying ratios of Soil A and Soil B in the mixed soil. As the proportion of Soil B increases in the mixed soil, the amount of large pores decreases, followed by that of medium pores, whereas the amount of small pores increases steadily. This phenomenon can be attributed to two reasons. First, small pores are the dominant pore type in Soil B; hence, the amount of small pores increases with increasing Soil B content in the mixed soil. Second, clay grains (<2 μm) are the dominant mineral content of Soil B. These grains fill in large and medium pores in the mixed soil.

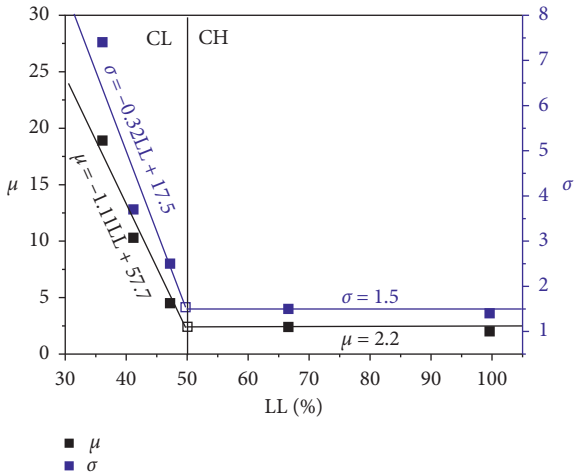

Figure 5: Relationship between normal distribution parameters and soil LL.

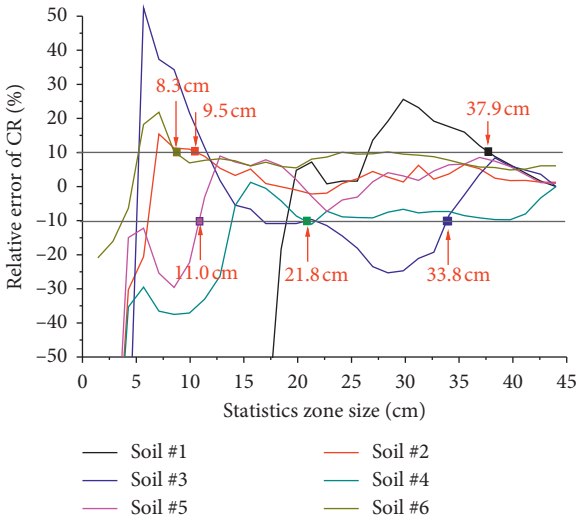

Figure 6: Relative error of CR under varying window sizes.

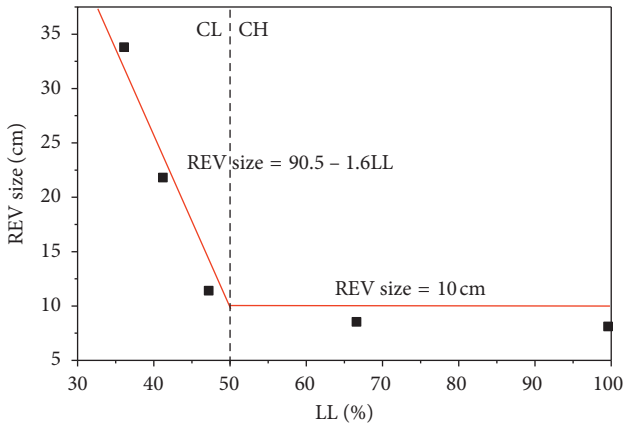

Figure 7: Relationship between REV and soil LL.

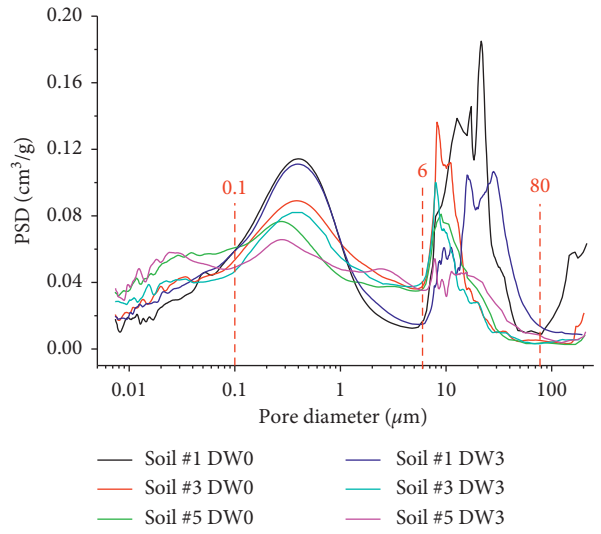

Figure 8: PSD in the CCLs before DW0 and DW3.

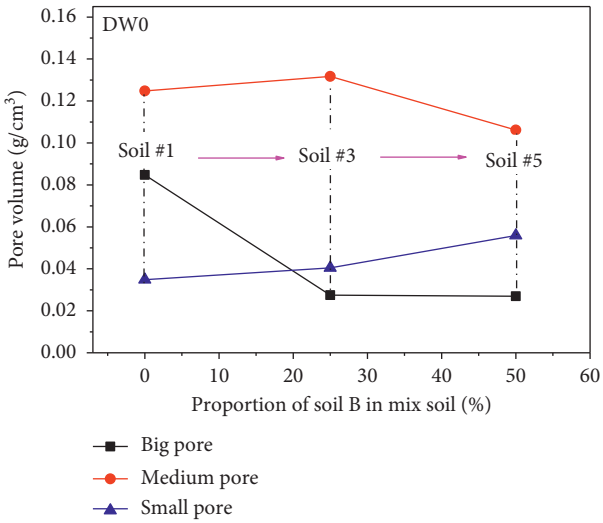

Figure 9: Different types of pore volume of three CCLs at DW0.

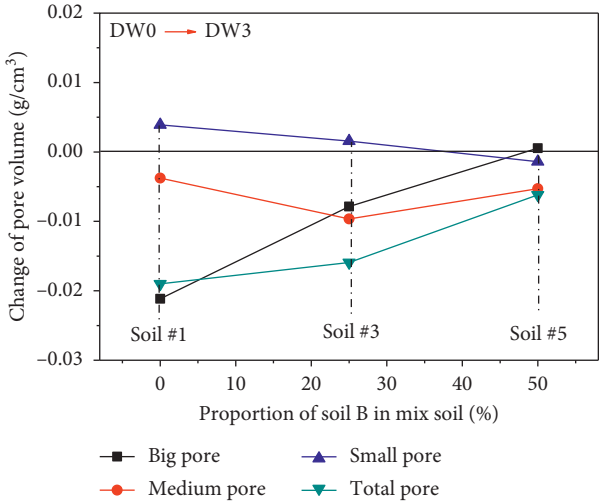

Figure 10: Pore volume change range of three CCLs from DW0 to DW3.

3.2.2. PSD in CCLs after Dry-Wet Cycles. Figure 10 shows the pore volume change range of three mixed soil samples before and after three dry-wet cycles. Each point in Figure 10 equals the pore volume of the soil sample before dry-wet cycles subtracts the pore volume after dry-wet cycles. The influence of dry-wet cycles mainly focuses on large pores for Soil #1, big and medium pores for Soil #3, and the medium pores for Soil #5. A trend in which pore size is mainly affected by dry-wet cycles decreases, as soil LL increases is observed. The cycles have minimal effects on the small pores of the three types of mixed soil. This condition is mainly attributed to the fact that effective stress is smaller on small pores than on large and medium pores because of suction cycles [5]. Furthermore, the deformation of pores in soil particles and crystal layers (small pores) is more difficult than in soil aggregates (large and medium pores). After three dry-wet cycles, the total pores in all three soil types decrease, thereby indicating that the shrinkage deformation of soil pores is not completely reversible during dry-wet cycles. The order of the change range of total pores in the three soil types is as follows: Soil #1 > Soil #3 > Soil #5. The range declines with an increase in soil LL and in Soil B content in mixed soil. This phenomenon is mainly attributed to the high bentonite content and strong self-healing capability of pore shrinkage.

3.3. Result and Analysis of CCL Permeability

3.3.1. Permeability Test Result. Table 5 presents the permeability test results of CCLs before and after three dry-wet cycles. At the same initial dry density, the initial permeability of the CCLs gradually decreases as Soil B content in the mixed soil increases before the dry-wet cycles. After three dry-wet cycles, the permeability of all the six CCLs increases from their initial values.

3.3.2. Effect of Dry-Wet Cycles on CCL Permeability. Figure 11 shows the change in CCL permeability as soil LL increases after three dry-wet cycles. As shown in Figure 11, the permeability ratio (K_3/k_0) initially increases and then decreases as soil LL increases, and LL at the peak value of K_3/k_0 is 36.6%. A similar result was confirmed in [11]. However, the permeability D-value ($K_3 - k_0$) decreases monotonously as soil LL increases. For low soil LL (<50%), linear relationships exist between permeability D-value and soil LL in a semilog coordinate system; the fitting result is shown in Equation (6). For high soil LL (>50%), permeability D-value change is inconspicuous with a mean value of approximately 1.67×10^{-8} cm/s:

$$\log(K_3 - k_0) = 1.719 - 0.197\text{LL}. \quad (6)$$

The initial permeability of the CCLs differs for each soil type even at the same initial dry density. The permeability ratio (K_3/k_0) is frequently used in many studies to assess change in soil permeability. However, an increase in permeability mainly results from desiccation cracks that do not close completely during wetting. Permeability after dry-wet cycles can be expressed as follows:

Table 5: Permeability test results of the six CCLs.

Soil number	Permeability (cm/s)		K_3/k_0	$K_3 - k_0$
	DW0 k_0	DW3 K_3		
Soil #1	6.75×10^{-7}	1.21×10^{-5}	17.9	1.14×10^{-5}
Soil #2	1.85×10^{-7}	5.61×10^{-6}	30.3	5.43×10^{-6}
Soil #3	6.32×10^{-8}	3.38×10^{-7}	5.4	2.75×10^{-7}
Soil #4	1.24×10^{-8}	4.25×10^{-8}	3.4	3.01×10^{-8}
Soil #5	2.21×10^{-9}	2.42×10^{-9}	1.1	2.10×10^{-10}
Soil #6	1.42×10^{-9}	1.48×10^{-9}	1.1	2.10×10^{-10}

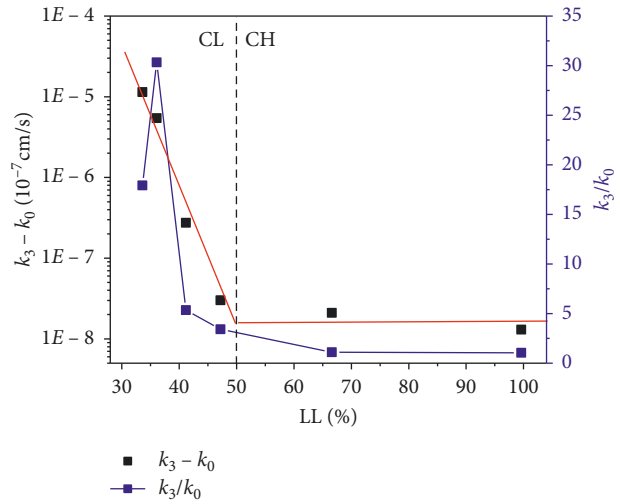

Figure 11: Change in CCL permeability as soil LL increases after dry-wet cycles.

$$K_3 = (1 - \alpha)K_M + \alpha K_C, \quad (7)$$

where K_M and K_C are the permeability of the CB area and crack area, respectively; and α denotes the CR.

Research in Wan et al. [3] shows that permeability change in the CB area is inconspicuous ($K_M \approx k_0$). Meanwhile, the crack area is significantly smaller than the CB area ($1 - \alpha \approx 1$). Thus, Equation (6) can be transformed into Equation (8) as follows:

$$K_3 - k_0 = \alpha K_C. \quad (8)$$

Equation (8) shows that using the D-value ($K_3 - k_0$) to evaluate the influence of dry-wet cycles on the permeability of different physical properties of CCLs is reasonable.

3.4. Relationship between Soil Structure and Permeability of CCLs. Two phenomena in CCL permeability are presented in this paper. First, CCL permeability decreases as soil LL increases before dry-wet cycles. Second, permeability D-value ($K_3 - k_0$) decreases monotonously as soil LL increases after three dry-wet cycles. Existing research has shown that CCL permeability is mainly dependent on the soil structure, including macrocracks and micropores. Before dry-wet cycles, the soil structure is only a soil pore structure because no crack is observed in the CCLs. Existing research has shown that a large pore functions as the seepage

channel and a medium pore functions as the connectivity channel of the seepage channel. As shown in Figure 9, large and medium pores decrease gradually as Soil B content increases in the mixed soil, which does not only reduce the seepage channel but also reduce pore connectivity, thereby resulting in a significant decrease in CCL permeability.

After three dry-wet cycles, the soil structure includes soil pore structure and cracks. Shrinkage cracks cannot completely close during wetting. Studies have already proven that the existence of preferential flow in a crack zone is the main reason for the considerable increase in CCL permeability, whereas the change in permeability in the CB zone is inconspicuous. The crack volume under the saturation condition is equal to the irreversible reduction of the total pore volume in the CCLs. As shown in Figures 10 and 11, total pore decrement and permeability D-value $(K_3 - k_0)$ decrease as soil LL increases. The mean crack width is also a primary factor that affects CCL permeability under the saturation condition. A linear relationship theoretically exists between permeability and the cube of crack width. Although the total pore volume of Soil #3 is slightly smaller than that of Soil #1, the mean crack width (total pore decrement divided by the total CL) of Soil #3 is evidently smaller than that of Soil #1; thus, the permeability D-value $(K_3 - k_0)$ of Soil #3 is clearly smaller than that of Soil #1.

4. Conclusion

The macro-microstructural damage and permeability change of six clay types under dry-wet cycles was studied in this work. The conclusions drawn are as follows:

(1) A piecewise linear relationship exists between crack parameters and soil LL, and the slope at LL < 50 is larger than the slope at LL > 50. The CB sizes of all the six CCLs correspond to normal distribution. As LL increases, the normal distribution parameters are reduced linearly and rapidly when LL < 50% but gradually when LL > 50%. For low soil LL, REV decreases linearly as soil LL increases. The linear fitting result is REV = 90.5 – 1.6 LL. For high soil LL, REV decreases slightly as LL increases. Therefore, setting REV as 10 cm for high liquid limit soil is appropriate.

(2) The bimodal PSD curves have pore sizes of 0.1, 6, and 80 μm in three troughs. Soil pores can be classified into three categories: large pores (>6 μm), medium pores (6 to 0.1 μm), and small pores (<0.1 μm). As clay content increases in mixed soil, the amount of large pores initially decreases, followed by that of medium pores. By contrast, the amount of small pores increases steadily. The influence of dry-wet cycles mainly focuses on large and medium pores, with minimal effects on small pores. A trend in which the effect of dry-wet cycles on pore size decreases as soil LL increases is observed. After three dry-wet cycles, total pore volume and its change range all decrease as soil LL increases.

(3) Before dry-wet cycles, the initial permeability of the CCLs gradually decreases as soil LL increases. After three dry-wet cycles, the permeability of all the six CCLs increases from their initial values. The permeability ratio (K_3/k_0) initially increases and then decreases as soil LL increases, and LL at the peak value of K_3/k_0 is 36.1%. However, the permeability D-value $(K_3 - k_0)$ decreases monotonously as soil LL increases. A linear relationship exists between permeability D-value and soil LL in a semilog coordinate system when LL < 50%, whereas the change in the permeability D-value is inconspicuous with a mean value of approximately 1.67×10^{-8} cm/s when LL > 50%.

(4) Before dry-wet cycles, the amounts of large pores (mainly seepage channels) and medium pores (connective channels of large pores) gradually decrease as soil LL increases, thereby significantly decreasing CCL permeability. Unclosed crack volume and mean width are two main factors that determine the increase in permeability after dry-wet cycles. After three dry-wet cycles, these two factors decrease as soil LL increases, thereby decreasing the permeability D-value $(K_3 - k_0)$.

Data Availability

The data used to support the findings of this study are available from the corresponding author upon request.

Conflicts of Interest

The authors declare that they have no conflicts of interest.

Acknowledgments

This research was supported by the Special Fund for Basic Research on Scientific Instruments of the National Natural Science Foundation of China (51625903, 51509245, and 41772342), Open Issues for State Key Laboratory of Geomechanics and Geotechnical Engineering (Z016001), and Open Issues for State Key Laboratory of Hydraulics and Mountain River Engineering (SKHL1508).

References

[1] J. H. Li, L. Li, R. Chen et al., "Cracking and vertical preferential flow through landfill clay liners," *Engineering Geology*, vol. 206, pp. 33–41, 2016.

[2] Z. L. Chen, *Technical Guideline for Projects of Municipal Solid Waste Sanitary Landfills (RISN-TG014-2012)*, China Architecture and Building Press, Beijing, China, 2012, in Chinese.

[3] Y. Wan, Q. Xue, and L. Liu, "Study on the permeability evolution law and the micro-mechanism of CCL in a landfill final cover under the dry-wet cycle," *Bulletin of Engineering Geology and the Environment*, vol. 73, no. 4, pp. 1089–1103, 2014.

[4] Q. Xue, H. J. Lu, Z. Z. Li et al., "Cracking, water permeability and deformation of compacted clay liners improved by straw fiber," *Engineering Geology*, vol. 178, pp. 82–90, 2014.

[5] Q. Xue, Y. Wan, Y. J. Chen et al., "Experimental research on the evolution laws of soil fabric of compacted clay liner in a landfill closure cover under dry-wet cycle," *Bulletin of Engineering Geology and the Environment*, vol. 73, no. 2, pp. 517–529, 2014.

[6] S. Krisnanto, H. Rahardjo, D. G. Fredlund et al., "Water content of soil matrix during lateral water flow through cracked soil," *Engineering Geology*, vol. 210, pp. 168–179, 2016.

[7] Q. Xue, Y. Zhao, L. Liu et al., "Study of thermo-hydro-mechanical-chemical coupling effect of catastrophe process of landfil," *Chinese Journal of Rock Mechanics and Engineering*, vol. 30, no. 10, pp. 1970–1988, 2011.

[8] M. A. Othman, C. H. Benson, E. J. Chamberlain et al., "Laboratory testing to evaluate change in hydraulic conductivity in compacted clays caused by freeze-thaw," in *Hydraulic Conductivity and Waste Contaminant Transport in Soil*, D. E. Daniel and S. J. Trautwein, Eds., pp. 227–253, ASTM STP 1142, Philadelphia, USA, 1994.

[9] A. A. Brian and C. H. Benson, "Effect of desiccation on compacted natural clays," *Journal of Geotechnical and Geoenvironmental Engineering*, vol. 127, no. 1, pp. 67–75, 2001.

[10] M. H. T. Rayhani, E. K. Yanful, and A. Fakher, "Desiccation induced cracking and its effect on hydraulic conductivity of clayey soils from Iran," *Canadian Geotechnical Journal*, vol. 44, no. 3, pp. 276–283, 2007.

[11] M. H. T. Rayhani, E. K. Yanful, and A. Fakher, "Physical modeling of desiccation cracking in plastic soils," *Engineering Geology*, vol. 97, no. 1-2, pp. 25–31, 2008.

[12] E. Drumm, D. Boles, and G. Wilson, "Desiccation cracks result in preferential flow," *Geotechnical News, Vancouver*, vol. 15, no. 1, pp. 22–25, 1997.

[13] G. H. Omidi, J. C. Thomas, and K. W. Brown, "Effect of desiccation cracking on the hydraulic conductivity of a compacted clay liner," *Water, Air, and Soil Pollution*, vol. 89, pp. 91–103, 1996.

[14] J. H. Li and L. M. Zhang, "Geometric parameters and REV of a crack network in soil," *Computers and Geotechnics*, vol. 37, pp. 466–475, 2010.

[15] Y. Wan, Q. Xue, Y. J. Chen et al., "Construction of consistent stability analysis model of landfill cover system and its application," *Chinese Journal of Rock and Soil Mechanics*, vol. 34, no. 6, pp. 1636–1644, 2013.

[16] C. Tang, B. Shi, C. Liu et al., "Influencing factors of geometrical structure of surface shrinkage cracks in clayey soils," *Engineering Geology*, vol. 101, pp. 204–217, 2008.

[17] Y. Y. Tay, D. I. Stewart, and T. W. Cousens, "Shrinkage and desiccation cracking in bentonite–sand landfill liners," *Engineering Geology*, vol. 60, pp. 263–274, 2001.

[18] D. L. Shear, H. W. Olsen, and K. R. Nelson, *Effects of Desiccation on the Hydraulic Conductivity Versus Void Ratio Relationship for a Natural Clay*, pp. 1365–1370, National Academy Press, Washington, DC, USA, 1993.